32nd URSI GASS, Montreal, 19-26 August 2017

Time Marching Simulation of Signal Propagation in Power Lines loaded with Non-Linear devices

Juan Becerra*(1), Felix Vega (1), and Farhad Rachidi(2)
(1) Electrical Engineering Department, Universidad Nacional de Colombia, Bogotá, Colombia
(2) EMC Laboratory, Swiss Federal Institute of Technology (EPFL), Lausanne, Switzerland

Abstract

In this paper, we present a time marching method for simulating signal propagation in power line networks loaded with non-linear devices. This method does not suffer from late time instabilities, since the time marching equations are obtained and stabilized in the Z-domain.

1. Introduction

The use of power lines for providing telecommunication services has attracted considerable interest due to the economic benefit resulting from the use of installed infrastructure. However, in-home power line networks are one of the most challenging media because the multipath effect over signal propagation is higher than in other networks (*i.e.* medium voltage), and non-linear behavior is introduced by devices connected to the power lines, which is often seen as dependence on time of the channel transfer function [1].

Hence, significant effort has been devoted to simulate power line networks in order to test the performance of different communication protocols. Nonetheless, simulations presented in the literature are based either on the linear periodic time variant (LPTV) model [2]–[5], which is an approximation of the non-linear nature of power line networks and it was validated up to 30 MHz [6], or on linear time invariant models [7], [8].

It is important to mention that current broadband power line communication (PLC) standards work up to 50 MHz for IEEE 1901 [9] and 80 MHz for G.hn 9960 [10]. Therefore, simulations of power lines networks with non-linear loads above 30 MHz based on the LPTV model may not be suitable.

In this paper, we extend the stable time marching (TM) method proposed in [11], which has been validated against FDTD, to simulate power line networks. Note that TM is able to capture the frequency dependence of the power lines and does not require any approximation of the non-linear loads.

The paper is organized as follows. Section 2 presents the formulation of the TM equations and the required modifications for achieving a stable simulation. Section 3 presents a simulation example. Finally, conclusions are given in Section 4.

2. Time marching equations

Consider that power line networks can be modelled as distributed multiport passive networks where each port may be connected to a source or load, such as the circuit shown in Figure 1.

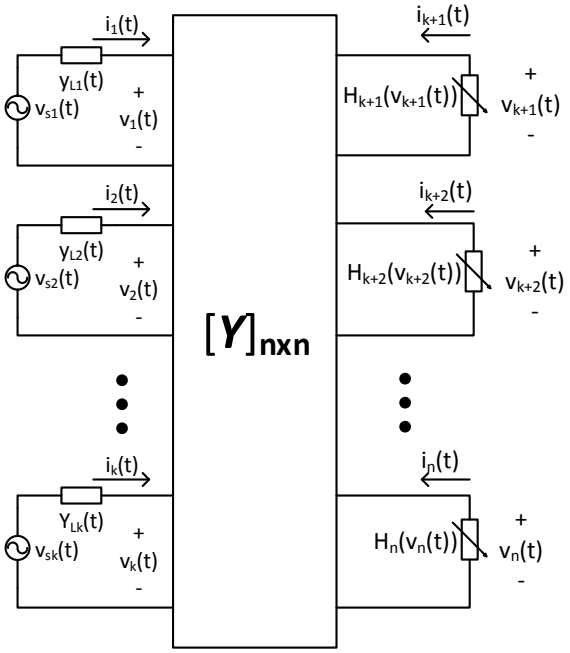

Figure 1. System with linear and nonlinear devices connected through a passive and distributed network.

In order to obtain the TM equations, the following methodology is applied:

1. Select the desired input and output variables.
2. Calculate the matrix transfer function.
3. Cast the equations into the Z-domain and discrete time domain.
4. Analyze the Z-domain equations and their discrete time domain counterpart in search of potential instability sources.

For the first step, we chose the variables in a way that the source admittances could be included into the multiport network. This leads to using (i) admittance parameters for representing the multiport network, and (ii) Norton equivalent of the voltage sources. This also allows to

represent the currents due to non-linear devices as sources whose impact will be explained later.

The relation between the Norton sources and the port voltages in the circuit of Figure 1 is given in the Fourier domain by:

$$\mathbf{C}(j\omega)=\left[\mathbf{Y}(j\omega)+\mathbf{L}(j\omega)\right]\mathbf{V}(j\omega) \tag{1}$$

where $\mathbf{L}(j\omega)$ is a matrix that contains the admittance of the linear loads, which is defined as follows:

$$L_{i,b}(j\omega)=\begin{cases} Y_{Li}(j\omega) & i=b\forall i\le k \\ 0 & others \end{cases}, \tag{2}$$

and the Norton currents, with the currents due to non-linear devices, are defined as:

$$C_i(j\omega)=\begin{cases} Y_{Li}(j\omega)V_{si}(j\omega) & i\le k \\ I_i(j\omega) & i>k \end{cases}. \tag{3}$$

where $V_{si}(j\omega)$ and $I_i(j\omega)$ are the Fourier a counterparts of the source voltages and port currents in shown in Figure 1, respectively.
The second step is straightforward and it is done by solving Equation (1) for the port voltages:

$$\mathbf{V}(j\omega)=\underbrace{\left[\mathbf{Y}(j\omega)+\mathbf{L}(j\omega)\right]^{-1}}_{\mathbf{A}(j\omega)}\mathbf{C}(j\omega) \tag{4}$$

Then, the following identity [11]

$$X(j\omega)Y(j\omega)\Leftrightarrow \Delta t X(z)Y(z), \tag{5}$$

is used to cast Equation (4) to the Z-domain, as follows:

$$\begin{bmatrix} V_1(z) \\ \vdots \\ V_n(z) \end{bmatrix}=\Delta t\begin{bmatrix} A_{11}(z) & \cdots & A_{1n}(z) \\ \vdots & \ddots & \vdots \\ A_{n1}(z) & \cdots & A_{nn}(z) \end{bmatrix}\begin{bmatrix} C_1(z) \\ \vdots \\ C_n(z) \end{bmatrix} \tag{6}$$

Thus, each voltage port can be rewritten as:

$$\begin{aligned} V_j(z)&=\Delta t\sum_{m=1}^{k}A_{jm}(z)C_m(z) \\ &+\Delta t\sum_{m=k+1}^{n}A_{jm}(z)C_m(z) \end{aligned} \tag{7}$$

And the discrete time domain counterpart is given by:

$$\begin{aligned} v_j(t_i)&=\Delta t\sum_{m=1}^{k}\sum_{l=1}^{i}a_{jm}(t_{i-l})c_m(t_l) \\ &+\Delta t\sum_{m=k+1}^{n}\sum_{l=1}^{i}a_{jm}(t_{i-l})c_m(t_l) \end{aligned} \tag{8}$$

The Norton currents in time domain are obtained from applying Equation 5 to Equation (3), as follows:

$$c_j(t_i)=\begin{cases} \Delta t\sum_{l=0}^{i}y_{Lj}(t_{i-l})v_{Sj}(t_l) & j\le k \\ \mathcal{H}_j\left(v_j(t_i)\right) & others \end{cases} \tag{9}$$

where the current through a nonlinear device is represented using a nonlinear operator $\mathcal{H}$ [12].

There are several aspects that are worth mentioning at this point:
(i) It can be seen from the Equation (8) that all the voltage port equations are coupled;
(ii) Every variable calculated through deconvolution is a potential source of instability [13];
(iii) The presence of nonlinear operators forces to perform a deconvolution to solve the current in the right side of Equation (8), or similarly, a division in Equation (7).

The first aspect can be addressed if delayed causality is considered, provided that every distributed system has a delay between the input and output ports [14]. This means that all the terms $a_{jm}(t_0)$ with $j\neq m$ in Equation (8) are equal to zero. Hence, the voltage port equations can be decoupled as long as delayed causality is enforced.

The second and third aspects mean that Equation (8) with $j>k$, will involve one deconvolution if delayed causality is enforced. Otherwise, there will be a deconvolution for each non-linear device. Thus, the deconvolution kernel will be $a_{jj}(t_i)$ or in the Z-domain, $A_{jj}(z)$.

In order to ensure stability of a time marching deconvolution, its kernel must be minimum phase [11]. Hence, it is mandatory to replace $A_{jj}(z)$ and $a_{jj}(t_i)$ by their minimum phase versions.

3. Example

Consider the topology shown in Figure 2. The transmission lines are formed by two parallel coated wires. The inner conductor radius is 4 mm, the wire coating thickness is 2 mm, and the distance between the two wires is 12 mm. The conductivity of the wires is 6.0×10^{7} S/m, whereas the conductivity and relative permittivity of the coating are 1.70×10^{-6} S/m and 3.19, respectively. The line lengths are: $S_1=5$ m, $S_2=20$ m, $S_3=15$ m, $S_4=10$ m and $S_5=8$ m.
The source v_{s1} represents the mains voltage with a peak voltage of 339.41 V at 50 Hz. The source v_{s2} is composed of two sinusoidal tones at 35 and 37 MHz with peak amplitudes of 100 mV. This allows the presence of intermodulation terms in the simulation.

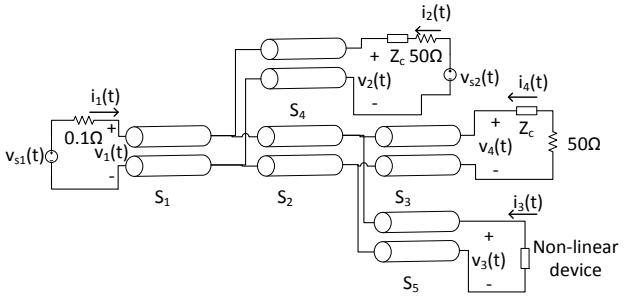

Figure 2. Four port network.

In addition, the source v_{s2} is meant to represent a PLC modem with a 50 Ω load output resistance. However, real life modems are equipped with a PLC coupler, which is represented by an impedance Z_c given by:

$$Z_c = \frac{1}{j\omega C} + j\omega L \tag{10}$$

where $C = 2.2$ μF and $L = 100$ nH. The capacitor blocks the mains voltage whereas the inductance represents the effect of the decoupling transformer [15]. Hence, the low and high cutoff frequencies of the coupler are respectively 1.44 kHz and 79.57 MHz. Note that the load at the Port 4 represents a PLC receiver.

It is important to mention that the non-linear behavior perceived by PLC signals is mostly due to the full wave rectifier in the input stage of devices in-home environments, with no Electromagnetic Interference (EMI) filter [16]. It is also claimed that the circuitry after the rectifier does not play an important role in the overall non-linear behavior [16]. Thus, we chose a full wave rectifier loaded with an RC circuit as the non-linear device, which is depicted in Figure 3.

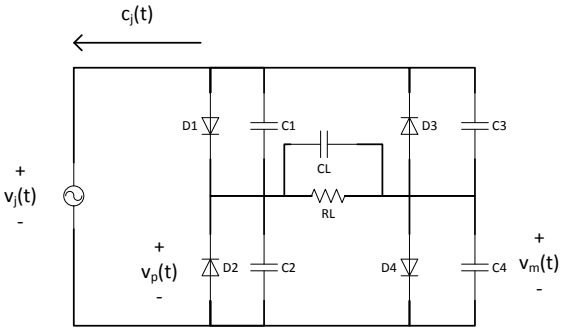

Figure 3. Full wave rectifier with diode capacitances.

The rectifier load parameters are $R_L = 512\Omega$ and $C_L = 100$ μF. The diodes are modeled with the following equation:

$$i_d(t) = I_s\left(e^{\frac{v_d(t)}{\eta v_t}} - 1\right) \tag{11}$$

where $I_s = 10.9774$ nA, $\eta = 1.78$ and $v_t = 25$ mV and $v_d(t)$ is defined under passive condition. The diode capacitances are given by:

$$C_d(v_d) = \tau_f \frac{I_s}{v_t}\left(e^{\frac{v_d(t)}{\eta v_t}} - 1\right) + \frac{c_{jo}}{\left(1 - \frac{v_d(t)}{v_{jo}}\right)^m} \tag{12}$$

where $\tau_f = 9.85376$ μs, $c_{jo} = 28.173$ pF, $v_{jo} = 0.507$ v and $m = 0.318$.

The resulting equation system that comes from the interaction between Equation (8) and the node voltages (shown in Figure 3) was solved by applying the Newton method. The equation system is not shown for the sake of brevity.

Finally, the transfer functions in $\mathbf{A}(j\omega)$ were sampled up to 40 MHz with 8193 samples and $a_{33}(t_i)$ was replaced by its minimum phase to achieve stability. It is important to mention that for a similar topology, the method of [11] requires about four million samples in the frequency domain to avoid time aliasing.

3.1. Simulation results

The port currents were calculated by:

$$i_j(t_i) = \begin{cases} \Delta t \sum_{l=0}^{i} y_{Lj}(t_{i-l})\left(v_{Sj}(t_l) - v_j(t_l)\right) & j \neq 3 \\ \mathcal{H}_j\left(v_j(t_i)\right) & j = 3 \end{cases} \tag{13}$$

and are shown in Figure 4. Then, the current $i_4(t)$ was used to calculate the power received by the "PLC modem", whose spectrogram is shown in Figure 5. Note that $i_4(t)$ is very large at the beginning due to the initial charge of the rectifier load.

It can be seen in Figure 5 that the intermodulation terms appear when the diodes start or stop conducting, for instance, at approximately 13.23 ms and 15.48 ms, respectively. This can be seen better with a comparison between the spectra obtained during the deactivation of the diodes and their normal conducting operation, which is shown in Figure 6. Note that a strong non-linear effect can be appreciated.

4. Conclusions

A suitable method for simulating non-linear effects on power lines has been presented. It provides stable simulation results and requires less samples than other stable time marching methods [11].

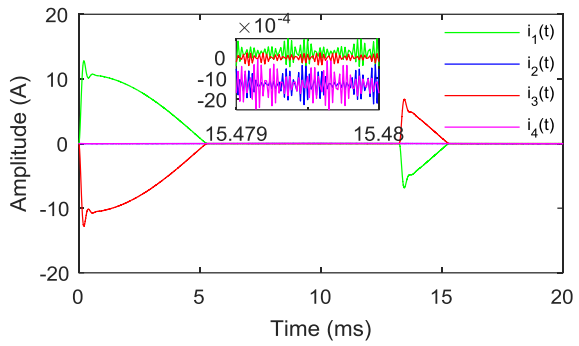

Figure 4. Port currents.

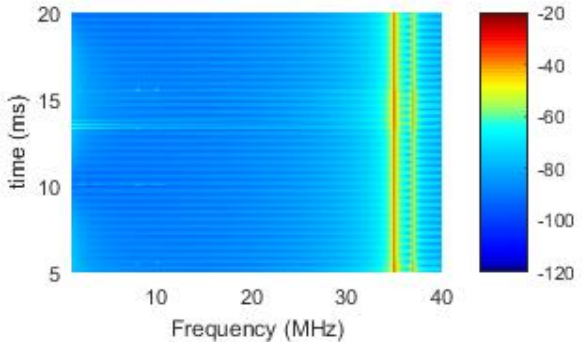

Figure 5. Power in dBm received in the 50 Ω load at port four.

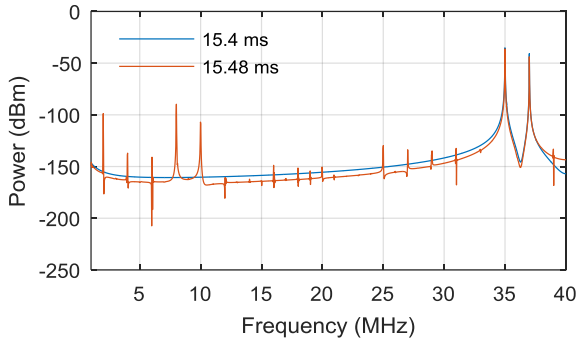

Figure 6. Power spectra at two different times.

5. References

[1] P. Amirshahi, F. Cañete, K. Dostert, S. Galli, M. Katayama, and M. Kavehrad, "Channel Characterization," in *Power Line Communications*, H. C. Ferreira, L. Lampe, J. Newbury, and T. G. Swart, Eds. John Wiley & Sons, Ltd, 2010, pp. 7–126.

[2] P. J. Pinero, J. A. Cortes, F. J. Canete, L. Díez, P. Manzanares, and J. Malgosa, "A Realistic HomePlug-AV Simulator for In-Home Network Services Planning," in *2011 IEEE Global Telecommunications Conference (GLOBECOM 2011)*, 2011, pp. 1–5.

[3] M. A. Tunc, E. Perrins, and L. Lampe, "Optimal LPTV-Aware Bit Loading in Broadband PLC," *IEEE Transactions on Communications*, vol. 61, no. 12, pp. 5152–5162, Dec. 2013.

[4] G. Marrocco, D. Statovci, and S. Trautmann, "A PLC broadband channel simulator for indoor communications," in *2013 17th IEEE International Symposium on Power Line Communications and Its Applications (ISPLC)*, 2013, pp. 321–326.

[5] F. Aalamifar, A. Schlögl, D. Harris, and L. Lampe, "Modelling power line communication using network simulator-3," in *2013 IEEE Global Communications Conference (GLOBECOM)*, 2013, pp. 2969–2974.

[6] F. J. Canete, J. A. Cortés, L. Díez, and J. T. Entrambasaguas, "A channel model proposal for indoor power line communications," *IEEE Communications Magazine*, vol. 49, no. 12, pp. 166–174, Dec. 2011.

[7] F. Versolatto and A. M. Tonello, "An MTL Theory Approach for the Simulation of MIMO Power-Line Communication Channels," *IEEE Transactions on Power Delivery*, vol. 26, no. 3, pp. 1710–1717, Jul. 2011.

[8] P. Achaichia, M. Le Bot, and P. Siohan, "Frequency Division Multiplexing analysis for point-to-multipoint transmissions in Power Line Networks," in *2012 16th IEEE International Symposium on Power Line Communications and Its Applications (ISPLC)*, 2012, pp. 230–235.

[9] S. Galli, H. Latchman, V. Oksman, G. Prasad, and L. W. Yonge, "Multimedia PLC Systems," in *Power Line Communications*, L. Lampe, A. M. Tonello, and T. G. Swart, Eds. John Wiley & Sons, Ltd, 2016, pp. 473–508.

[10] K. Dostert *et al.*, "Digital Transmission Techniques," in *Power Line Communications*, L. Lampe, A. M. Tonello, and T. G. Swart, Eds. John Wiley & Sons, Ltd, 2016, pp. 261–385.

[11] J. Becerra, A. Tatematsu, F. Vega, and F. Rachidi, "Stable simulation of nonlinearly loaded lossy transmission lines with time marching approach," in *2016 IEEE International Symposium on Electromagnetic Compatibility (EMC)*, 2016, pp. 261–266.

[12] F. M. Tesche, "On the Analysis of a Transmission Line With Nonlinear Terminations Using the Time-Dependent BLT Equation," *IEEE Transactions on Electromagnetic Compatibility*, vol. 49, no. 2, pp. 427–433, May 2007.

[13] J. E. Michaels, "Fundamentals of deconvolution with applications to ultrasonics and accoustic emission," Cornell, 1982.

[14] R. Mandrekar and M. Swaminathan, "Causality enforcement in transient simulation of passive networks through delay extraction," in *9th IEEE Workshop on Signal Propagation on Interconnects, 2005. Proceedings*, 2005, pp. 25–28.

[15] C. J. Kikkert, "Coupling," in *Power Line Communications*, L. Lampe, A. M. Tonello, and T. G. Swart, Eds. John Wiley & Sons, Ltd, 2016, pp. 223–260.

[16] M. Antoniali and A. M. Tonello, "Measurement and Characterization of Load Impedances in Home Power Line Grids," *IEEE Transactions on Instrumentation and Measurement*, vol. 63, no. 3, pp. 548–556, Mar. 2014.